ISSN 1064-2293, Eurasian Soil Science, 2018, Vol. 51, No. 7, pp. 814–826. © Pleiades Publishing, Ltd., 2018.
Original Russian Text © O.P. Yermolaev, A.M. Gafurov, B.M. Usmanov, 2018, published in Pochvovedenie, 2018, No. 7, pp. 870–883.

DEGRADATION, REHABILITATION, AND CONSERVATION OF SOILS

Evaluation of Erosion Intensity and Dynamics Using Terrestrial Laser Scanning

O. P. Yermolaev[a], *, A. M. Gafurov[a], and B. M. Usmanov[a]

[a] *Kazan Federal University, Kazan, 420008 Russia*

**e-mail: oyermol@gmail.com*

Received July 6, 2017

Abstract— A new method of instrumental measurement of the intensity of rill and linear erosion on slopes by the method of terrestrial laser scanning is proposed. This method was tested on four plots in 2012–2016 with the use of Trimble™ GX, Trimble™ VX, and Trimble™ TX8 laser scanners. The terrestrial laser scanning is characterized by a high precision and rapidity, which could not be previously achieved by other devices. It has a number of advantages: registration of various types of erosion of temporary water streams; measurements from a distance without the disturbance of the studied surface and providing the safety of works; and calculations of morphometric parameters of slope using a high-precision digital model of topography. The given examples show that this approach may be applied to assess the denudation-accumulative balance of the moved soil material on slopes, to determine the dynamics of amount of deposits on different parts of a slope as a result of different kinds of surface runoff, and to identify spatial regularities of the formation of the network of rills and gullies. In addition, laser scanning makes it possible to perform an integral assessment of the combined impact of the entire combination of exogenous processes developed on slopes and affecting the soil cover. The observations on test plots showed a rather great role of autumn rains in the total soil loss from erosion. The data obtained were used as the basis for the elaboration of practical recommendations concerning the survey organization and monitoring of erosion with the use of laser scanning.

Keywords: field laser scanning, soil erosion, mapping

DOI: 10.1134/S1064229318070037

INTRODUCTION

Erosion processes on slopes (soil loss and gully formation) have been studied for a long time all over the world. There are a lot of approaches for the assessment of erosion intensity. Their reviews are given in numerous published works of Russian and foreign scientists [2–6, 26]. Nevertheless, problems of the quantitative evaluation of erosion intensity in different parts of the modern hydrographic network, which includes erosional forms of different morphologies created by the surface runoff, have not been solved. In fact, none of the existing methods provides comprehensive data on erosion rates and their spatial–temporal dynamics on different parts of slope. This complicates the development of reliable erosion models and measures to control this process. The difficulties of the determination of slope erosion intensity are related, on the one hand, to a very small (less than 1 mm/yr) amount of eroded soil in the area of rill erosion, and, on the other hand, to extremely strong destruction of soils as a result of gully erosion [4]. The difficulties of erosion survey are enhanced by a large number of factors, which affect it, and a great variability of the process in space and time. At present, new high-precision instrumental methods of erosion monitoring appear (unmanned aerial vehicles and geodetic equipment). Their potential should be evaluated, and adequate methodological approaches should be developed.

The aim of this work was to elaborate a method of the quantitative evaluation of the intensity and dynamics of erosion by temporary water streams on slopes with the use of field laser scanning.

OBJECTS AND METHODS

We studied erosional processes related to the activity of temporary water streams on slopes, including rill, channel, and gully erosion. The works were performed on test plots in the forest-steppe zone in the east of the Russian Plain (within the Republic of Tatarstan).

Attention to the laser scanning method is related to a number of its fundamental advantages over other methods of erosion assessment: fast measurements without loss of accuracy, elaboration of a complete digital model of the object; performance of the work under any lighting conditions; possibility of survey of remote and complex objects, full automation of measurements, measurement of geometric parameters on the obtained digital 3D mode, and storage of 3D data on the object in a digital form.

The review of published works shows that the assessment of the intensity of exodynamic processes with the use of laser scanning systems appeared early in the 2000s. These systems were first tested for determining the rate of landslide processes. For example, in 2008, a group of Spanish scientists under the supervision of O. Monserrat was the first to perform the terrestrial laser scanning (TLS) to measure deformation on landslide slopes [24]. Georeferencing of the scans obtained in different periods was performed using the approach of least squares adapted for matching 3D surfaces [18]. In 2005–2009, scans made in the crater of the Vesuvius Volcano in different periods were matched by Italian scientists by the method of Iterative Closest Point (ICP) [29].

In 2014, a group of Poland scientists proposed a different approach for registration of scanning data. A network of reference points was made on the ground to register scans. Coordinates of the reference points were determined by the differential global positioning system (DGPS) [22]. The registration accuracy with the account for the error of the DGPS receiver was 26 cm. Laser scanning for monitoring of gully processes was performed by the same group of scientists in 2015 in conventional coordinates, which made it possible to increase the registration accuracy of scans by two orders [21]. Similar investigations of 2008–2010 belong to the Jiménez-Perálvarez scientific group (Spain) [27] and to Swiss scientists (2012) under the leadership of M. Franz [17]. The specific feature of these investigations is the use of the ICP algorithm in addition to fixation of coordinates of reference points for georeferencing of the scans to improve the results. The combination of these technologies ensured the georeferencing accuracy of 11 mm in plan and 17 mm in height. In all the works with the use of TLS, the main attention is reasonably paid to the scanning technology and assessment of the accuracy of the results.

Thus, the use of various georeferencing methods makes it possible to achieve centimeter accuracy of the scans' matching. This error is permissible at studying landslide processes because of great changes on slopes. However, it is insufficient for studying low-rate exogenous processes (including rill and channel erosion), which create morphological forms of small sizes. Laser scanning of exogenous processes is being actively developed in Western Europe, Japan, China, Brazil, the United States of America, and some other countries. The survey data on exodynamic processes obtained by this method were presented at numerous scientific forums: the General Assembly of the European Geosciences Union (Vienna) in 2012–2017 (section Landslide Hazards), the VIII International Conference on Geomorphology (Geomorphology and Sustainability, Paris, 2013), the International Symposium on Gully Erosion in 2016 (United States), etc. Most of reports describe TLS application for the assessment of high-speed (from the first centimeters and higher) exogenous processes, which result in considerable denudation (landslides, horizontal shifts of the channels of mountain rivers, movement of mountain glaciers, eolian accumulation, gully formation, etc.). In all the works, the main attention is paid to survey approaches and accuracy of the data obtained.

Despite the great number of studies devoted to monitoring of exogenous processes with the use of TLS, the works on scanning of rill erosion are few in number, because sub-millimeter accuracy of the registration of data of repeated surveys is required [1]. This problem is solved by foreign scientists only in laboratory [11, 14]. In 2004, German scientists performed TLS with millimeter accuracy, which was impossible in preceding periods, and elaborated millimeter-resolved 3D digital topography models (DTR) [30]. Data obtained by TLS represent a reliable source of information on microfeatures of topography upon calculation of soil loss by erosion models (for example, the SIBERIA model [19]). The use of reference benchmarks enables inter-seasonal and annual surveys of the same plot with millimeter accuracy [1, 9].

The efficiency of TLS for the evaluation of erosion intensity was confirmed by numerous works of foreign scientists [8, 13, 15, 20, 23, 25, 33–35]. High performance (up to one million points per second) [32] and accuracy [15, 16] of scanners was pointed out. At the same time, rill and flow erosion was not evaluated by TLS, or the works were at the stage of selection of the experimental plots for subsequent survey. Published data on erosion in the periods of snowmelt runoff measured with the use of TLS are absent. There are no generalized TLS data on erosion and accumulation of soil material on plowed slopes.

Despite the wide use of TLS in foreign investigations, the works on the assessment of rill erosion by this method are virtually absent in Russia. In this context, we paid special attention to methodological aspects of the use of TLS technique for the evaluation of soil erosion by temporary water flows.

The method for erosion determination by TLS was elaborated on test plots of small area. Such experiments are used all over the world, because only the work on a large scale makes it possible to take into account a great number of various parameters affecting the scanning accuracy.

Observation plots. A part of denuded left slope of the Kazanka River valley was taken as a test plot (plot Kazanka) (Fig. 1a). This 18-m-long plot was located on the southwestern slope; it had an average steepness of 31.5° (the amplitude of heights was 9 m). The cross-section of the slope represented a straight line. The total area of the plot was 0.07 ha, and the scanned part without vegetation had an area of 35 m^2. The human-made soil layer (peat) was underlain by heavy colluvial loams. We chose two sectors of observation (A and B), which were divided into three experimental fragments on the top, middle, and low parts of the slope. These plots were chosen, because the network of rills was

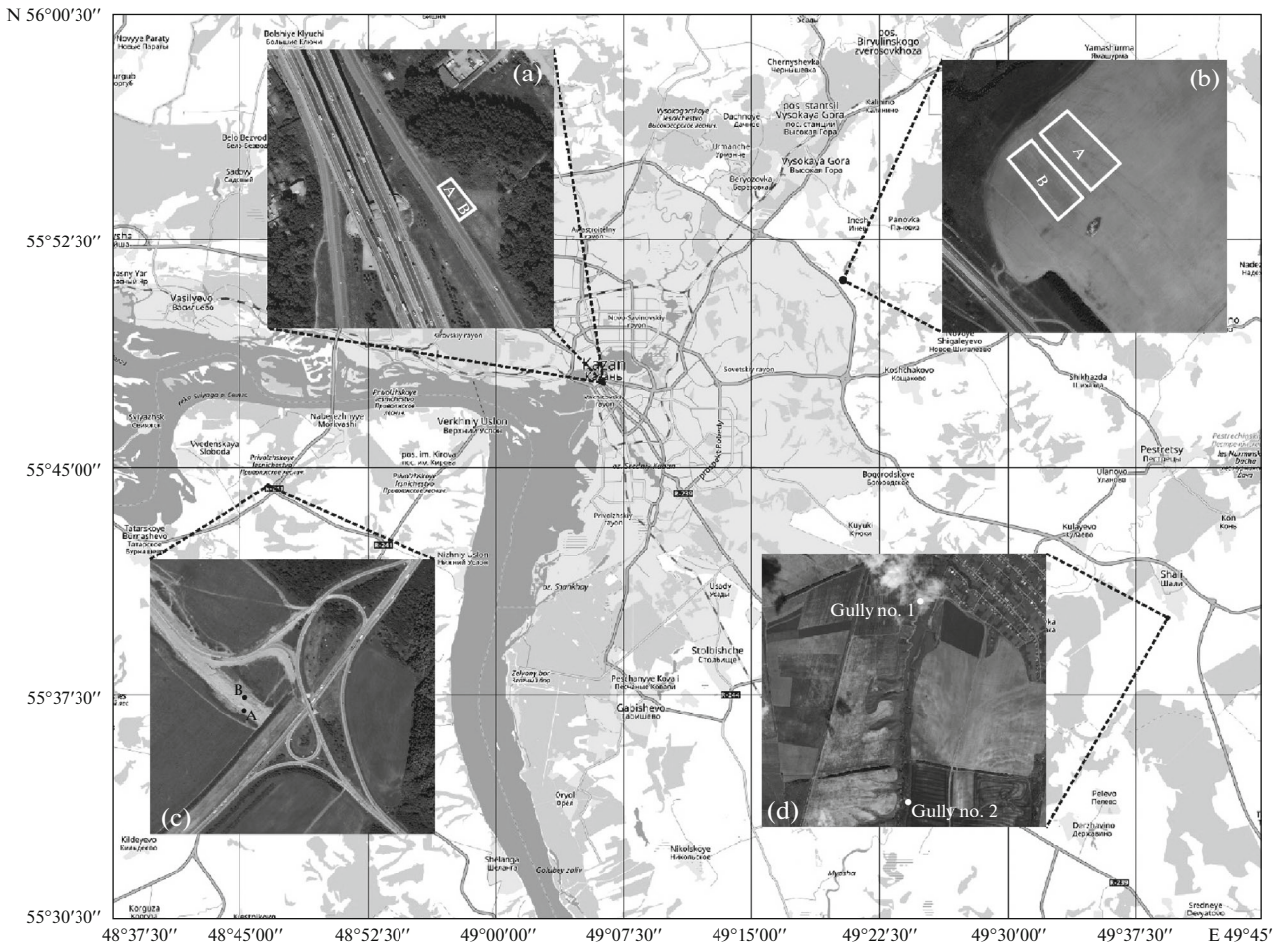

Fig. 1. Observation plots Kazanka (a), Chebaksa (b), Innopolis (c), and Shali (d).

clearly expressed on them, and the grass cover was absent. The latter feature is a necessary condition for erosion survey by the TLS method. The area was scanned after the end of snowmelt runoff and after heavy rains, or after the period with a great precipitation layer. The observation series here were the longest (2012–2016), and they were obtained with the use of various scanners (Trimble™ GX, Trimble™ VX, and Trimble™ TX8).

The TLS approach for erosion determination was tested on agricultural lands in 2015. The observations were performed on arable land in the period of surface runoff after heavy rain in the basin of the Kinderka River (Chebaksa plot) in Prikazanskii district. The soil cover of the field on the northwestern slope of 5.52° consisted of the heavy loamy light gray forest soils (Luvisols). We scanned two plots with morphologically well pronounced rills and channels of up to 30 cm in width (Fig. 1b). The appearance of young perennial grasses prevented the organization of a long series of repeated observations.

To determine erosion intensity on bedrock outcrops, a plot on the right bank of the Volga River, 2 km to the south of the city of Innopolis (Innopolis plot) in summer 2016. We studied two 10-m-long segments of slopes of the northeastern and southwestern aspects with a rectilinear shape of the cross-sections (Fig. 1c). The slopes were completely denuded, had no soil cover, and were composed of clayey–marly deposits of the Late Permian age.

Two gullies located on the left and right slopes of the Temev Ruchei River valley (the right tributary of the Mesha River) were chosen as test plots for scanning gully erosion (Fig. 1d). Gully 1 was located on the left bank of the valley cutting the colluvial–solifluction loams, and gully 2 was located on the right bank of the river and exposed the clayey–marly Upper Permian deposits.

Scanning devices. We used various terrestrial scanning devices to find the one with optimal measurement accuracy, convenient for work in the terrain conditions, and having adequate cost. We tested a Trimble™ VX spatial station with laser scanning (10–15 points/s) and Trimble™ GX (5000 points/s) and Trimble™ TX8 (1000000 point/s) laser scanners.

The technology of terrestrial laser scanning consists of fixation of the direction of laser beam and measurement of distances to a large number of points located on the scanned object. As a result, we obtain a cloud of points, which contain information on the X, Y, and Z coordinates, signal intensity, and actual color of the point. The angles are not measured, but are predetermined by the turn of the mirror and are simultaneously registered by a recorder. All measurements are performed in the mode of continuous observation; the scanning density depends on the distance and may be tenths of millimeter. The scanning data are used for plotting a 3D model, which may be converted into computer-aided design systems (CAD) and geographic information systems (GIS).

The refinement of the technique was started with use of a Trimble™ GX 3D laser scanner. Its main advantage is the possibility to focus laser beam on the object. As a result, the device is capable to scan small objects from a considerable distance (up to 350 m). The mode of multiple measurements provides higher accuracy of the GX laser scanning system; the distance to the object is calculated as the mean of multiple measurements. The scanning data are registered by special flat and spherical marks. The disadvantages of the device include the absence of energy supply source and impossibility of operation at temperatures below zero.

The main advantage of Trimble™ TX8 device is the high scanning speed: to 1000000 points/s. Scanning lasts from 1 to 10 min depending on the chosen mode. The marks are registered after scanning, so the placement of special marks on points with the known coordinates is the most time-consuming at scanning. The distance to marks should not exceed 30–40 m for the successful detection by the program, but the possibility to organize permanent benchmarks at such distance is absent in the terrain conditions because of the risk of their destruction at plowing. This procedure was performed by spatial station. Coordinates of the station were determined by resection, and then the points, on which special marks were placed, were excluded. A high cost is an essential disadvantage of this device.

Trimble™ VX is a robotic spatial station. This is a multifunctional device, which may be used not only for topographic survey with a geodetic accuracy but also for creating 3D clouds of points and for high-resolution photography. Our study suggests that this is the optimal device for laser scanning of erosion of temporary water streams from the point of view of the data quality, operability, and cost. Its main advantage is the high accuracy of registration with a possibility of geodetic substantiation of the accuracy. This is especially important at studying rill erosion, which is characterized by small (from the tenths of a millimeter to several millimeters per year) denudation and accumulation rates. Taking into consideration that soil erosion should be measured for the system of linear washouts (rill-erosion component), this device is optimum for this kind of survey. The maximal resolution at scanning is 1 cm, which corresponds to the resolution taken by us at the application of the laser scanner. It may be also used for the survey of gullies, where millimeter accuracy is not required. The registration errors at the use of modern high-speed scanners may be only calculated upon data treatment after scanning, while the positioning accuracy of Trimble™ VX is estimated just before scanning. Photographs may be used for the comparison of parameters for different dates and formation of textures at modeling. In addition, this is a rather compact and inexpensive device with the system of independent power supply, which gives it an advantage over the Trimble™ GX scanner. Disadvantages of the device include low scanning speed, which results in the increase in the operation time on the plots. In this connection, this scanner is recommended for survey at small distances from the object.

METHODS OF SCANNING AND DATA PROCESSING

The elaboration of the order of scanning procedures, beginning from the selection of the plot optimum for scanning to the determination of quantitative parameters of erosion, was the main aim of the study of erosion rates and dynamics by TLS. A special attention was paid to a high scanning accuracy and coordination of data of repeated surveys to minimize errors at further data processing. The approach was developed with due account for specific features of various 3D scanners and may be used for all their types.

The major stages of the procedure to monitor erosion control are common for all the used scanners.

—*Choice of the plot*. The plot should have morphologically pronounced evidences of rill and gully erosion in order to estimate changes in the structure and morphology of these elements upon repeated observations. It has been demonstrated that the evaluation of sheet erosion is rather difficult, because changes in nano- and microfeatures of topography of denuded soil may be determined by the factors, which are not related to erosion (the type of land cultivation by field machines, solifluction and landslides in the period of the snowmelt runoff, etc.). We cannot determine the role of sheet erosion in the data obtained for the layers of depletion and accumulation on the studied plot. The absence of continuous plant cover on the plot is another important condition. Vegetation is opaque for laser beam and prevents relief scanning. This condition determines the best period of scanning of plowed slopes: spring after snowmelt runoff and after spring plowing of fields prior to the appearance of young crops. In addition, there should be a place on the plot for equipment installation, which should ensure its safety and stable operation. There should be also a place for a network of benchmarks for reliable coordi-

Table 1. TLS data for May–June 2015 (Kazanka plot, sector B)

Slope part	S, m^2	V_-	V_+	V_+-V_-	i_-	i_+	Δi	E, m^3/ha
		m^3			mm			
Upper	3.70	0.05	0.003	−0.04	−12.56	0.86	−11.70	−117.00
Middle	3.69	0.03	0.004	−0.02	−6.88	1.08	−5.80	−58.02
Lower	3.71	0.02	0.05	0.03	−5.14	13.95	8.81	88.11
Total slope	11.11	0.09	0.06	−0.03	−8.19	5.31	−2.88	−28.80

Here and in Tables 3–6: S is the measured plot area; V_+ is the volume of accumulated material; V_- is the volume of eroded material; i_+ is the accumulated layer; i_- is the eroded layer; Δi is the predominant process (erosion or accumulation); E is the volume of eroded–accumulated material. Sign (+) signifies sediment accumulation, and sign (–) signifies erosion.

nation of scans with one another upon repeated observations.

—*Installation of the equipment and scanning*. The scanning equipment is installed so that the laser scanner is located in front of the examined slope subjected to erosion on a support. The height of the support should provide the maximal coverage of the studied part of the area (object) by one scan. The scanner should be aligned with the use of a tribrach. Testing of the approach in terrain conditions has shown that when the study of erosion processes requires high precision of measurements, the horizontal and vertical position of the station should be strictly fixed. The displacement of the station at repeated scanning will cause a change in the scanning angle, which is undesirable at studying small elements formed by erosion. For the geodetic substantiation of scanning data, it is necessary to create at least three reference points with the known coordinates or in the conditional coordinate system in a way that the scanner is found inside the formed perimeter. For scanner adjustment in the coordinate system, it is recommended using geodetic prisms and/or special benchmarks proposed by the producer of the scanning equipment and installed on a support with the tribrach. The height of the benchmark should be measured at each scanning. The mean square deviation at the adjustment of the scanner should not exceed 1 mm. Special benchmarks are usually placed by pairs on a circle approximately each 90°. The experience has shown that this dislocation and quantity of benchmarks make it possible to reduce the time for their setting, prepare the working horizontal and vertical scanning scheme, and scan the terrain. The resolution of plot scanning is no less than 3 mm per 10 m but no more than 10 mm per 10 m. A panoramic (360°) photography of the area with the use of the camera installed into the device is recommended. This will make it easier to correlate the cloud of points with the scanned surfaces and provide more precise visual determination of changed areas and the texturing of surfaces.

—*Data processing*. The scans are used for the construction of a digital elevation model (DEM) with the grid interval equal to the scanning step. The clouds of points should be processed. The world experience has shown that the most efficient software for processing these data include Golden Software Surfer [10], Innov Metric Software Polyworks, Maptek I-Site Studio, Leica Cyclone, Faro Scene, JRC 3D Reconstructor [8], and Riegl Riscan PRO [28]. The import, stitching of scans made at different stations, segmentation, and removal of artifacts were performed with the use the Trimble™ RealWorks software. The stitching of scans was checked by the following formula [31]:

$$\sigma = \sqrt{\frac{1}{M}\sum_{p=1}^{M}(\delta_p - \mu)^2}, \quad (1)$$

where σ is the standard deviation of stitching error; M is the amount of stations; δ_p is error in X, Y, and Z; and μ is the mean error for all points at all the stations (calculated individually for X, Y, Z).

To minimize the errors, the objects-artifacts (plants, power line poles, etc.) must be eliminated in a special utility program with the use of automatic filters [31] or manually. Each of the approaches has its advantages and disadvantages, so both methods should be used for the best results.

The clouds of points cleaned of artifacts were exported to the Golden Software Surfer to construct and analyze the DEM. At its construction, the approach of "inverse distance to a power" was used. It combines the speed and the greatest possible accuracy at reconstruction of the surface [10].

With respect to the slope extension, the constructed DEM was divided into three equal sections representing the upper, middle, and lower parts of the slope. However, the total areas of these sections were not equal, because lands without plant cover were only taken into consideration (Table 1). As a result, we could evaluate the spatial variability of erosion on the plots in different periods of time. Rill erosion was determined by the models. For this, maps of local runoff directions were compiled in the automatic mode and then were used for the compilation of the maps of washout processes. The threshold size of the grid was experimentally determined in order to reflect rill washouts more than 1 cm deep. The map of the net-

work of rills was then used to delineate the areas without washouts: buffer zones were specified from the thalweg of washout with respect to its depth. They were then subtracted from the initial DEM. The gaps were filled in by the approach of linear interpolation. The DEMs were used for the assessment of quantitative parameters in the period of slope reformation.

The maps of rill washouts were used for the calculation of their total length and the density of the rill network in the ESRI ArcMap software:

$$D = L/S, \quad (1)$$

where D is the density of the rill network (m/m^2); L is the total length of the rill network (m); and S is the plot area (m^2).

For the calculation of volumes of eroded and accumulated material and the compilation of maps of surface differentiation, DEMs constructed for different time periods were subtracted. The quantitative parameters of erosion–accumulation processes were determined for each fragment (upper, middle, and lower parts of the slope). The Volume instrument of the Golden Software Surfer was used. This utility program also enabled calculation of the areas of the plots. Then, the layer of erosion and accumulation (mm), the predominant process, and the volume of eroded and accumulated material were calculated for the area of the plot:

$$i_- = \frac{V_-}{S} \times 1000, \; i_+ = \frac{V_+}{S} \times 1000, \quad (3)$$

where i_- is the eroded layer, mm; i_+ is the accumulated layer, mm; V_- is the eroded volume, m^3; V_+ is the accumulated volume, m^3; and S is the plot area, m^2.

$$\Delta i = \frac{V_+ - V_-}{S} \times 1000, \quad (4)$$

where Δi is the predominating process, mm.

$$E = \frac{V_+ - V_-}{S} \times 10\,000, \quad (5)$$

where E is the volume of eroded–accumulated material per unit area (m^3/ha).

These calculations after each observation enabled us to quantify the dynamics of losses of soil on the plowed land after the surface runoff on the slope.

In addition to quantitative characteristics, the graphical representation of data was used for more comprehensive evaluation of erosion processes on the studied plot. Compilation of differential maps, lengthwise and transvers profiles (Figs. 2, 3) for the most typical linear washouts, and the analysis of the horizontal structure of rill network for the assessment of its transformation (Fig. 4, Table 2) were performed.

The methods of laser scanning of gullies are better elaborated, and the organization of our observations was based on the experience of foreign scientists [20, 25, 35]. For registration accuracy of repeated observations, a network of ground reference points was set, and the first adjusting scanning was made in autumn 2015.We performed scanning three times in 2015–2016 for each of the gullies to record volume changes after the periods of snowmelt and rainstorm runoff. Scanning by a Trimble™ VX robot spatial station provided the registration error, which did not exceed 1 mm. The scanning resolution of gully surface was 5 cm per 8 m, and the scanning density was 185 points/m^2. Such artifacts as excluded points and vegetation were eliminated from the clouds of points with the use of the Trimble™ RealWorks software. The clouds were exported to the Golden Software Surfer to construct the DEM with the grid cell size of 5 cm and to calculate the volume changes of the studied object.

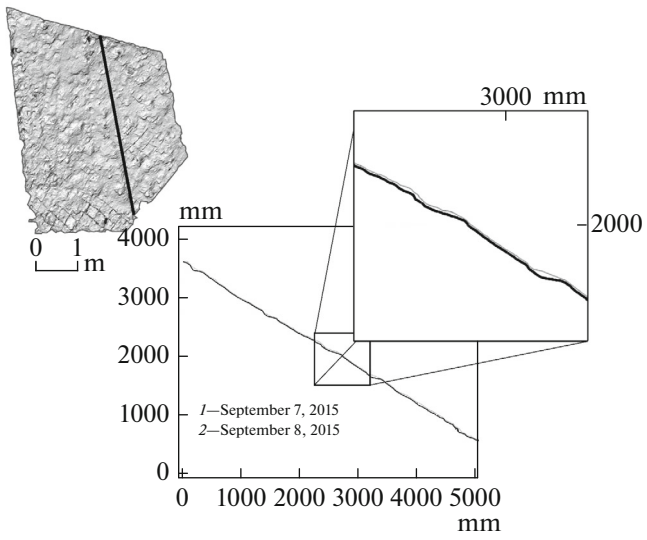

Fig. 2. Lengthwise profile of slope and its location by the example of plot B scanned on September 7–8, 2015.

RESULTS AND DISCUSSION

The observation data and their format may be shown by the example of the test plot located on the left slope of the Kazanka River valley (Kazanka plot). As mentioned above, two sectors of scanning were chosen there (A and B). The parameters were measured after snowmelt runoff and after each heavy rain or rain with a large precipitation layer. Data on precipitation were taken from the Kazan University meteorological station.

A comparison of point clouds of repeated scanning on test plots makes it possible to identify the beginning and further development of erosion. Let us discuss some observation data. In 2014, the first TLS was performed on April 12 after the snowmelt runoff. Numerous mud slides were formed on the slope because of its great steepness, high water content, and the specific composition of the underlying material. Their origin was related to solifluction and ground creep. The

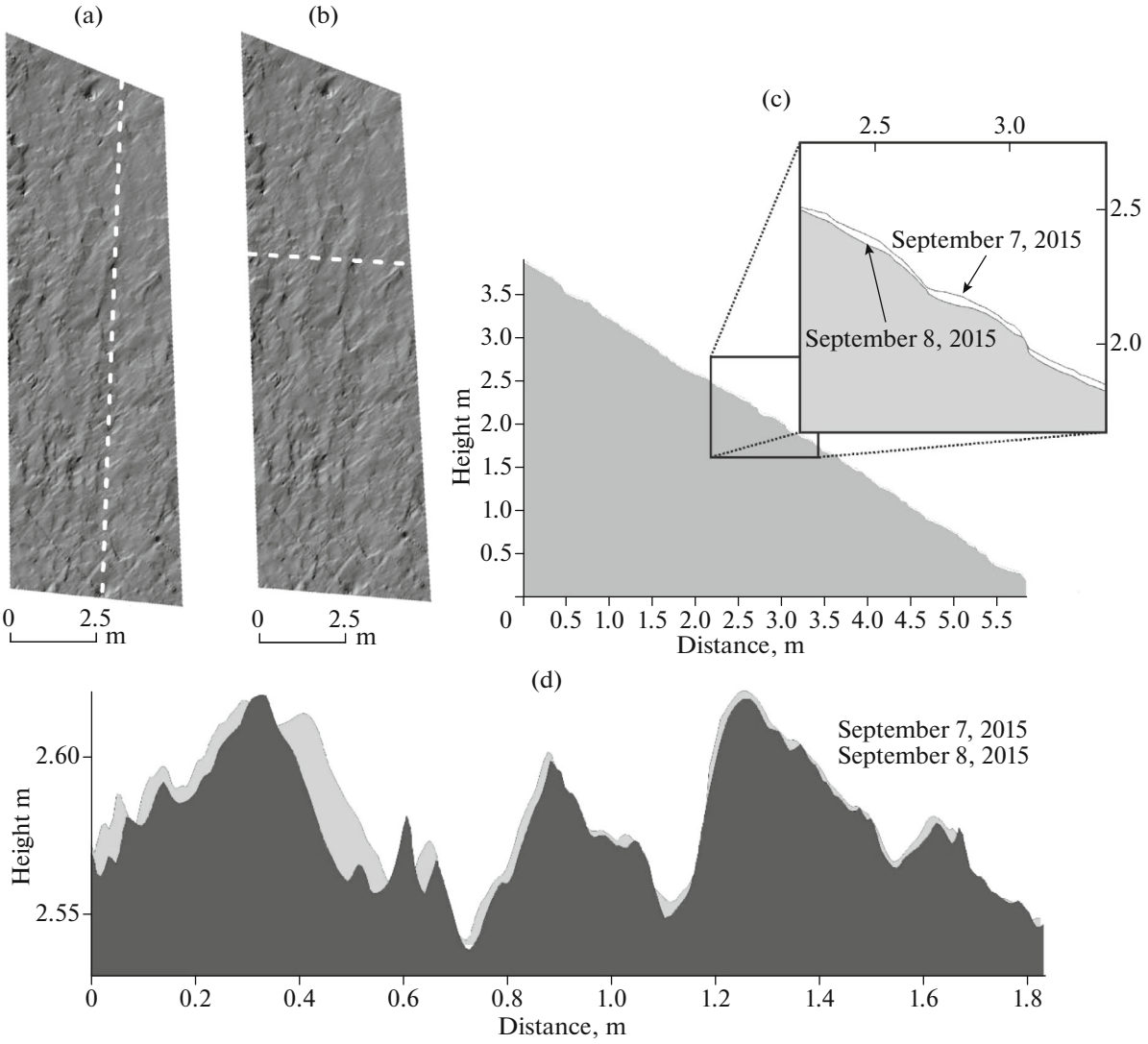

Fig. 3. Lengthwise (a, c) and cross (b, d) profiles of sector B (Kazanka plot) before and after an extremely heavy rain in 2015.

thickness of continuous snow cover in March (March 6–9, 2014) was 33–53 cm, water reserve in snow (with the bulk density of 0.3 g/cm^3) varied from 120 mm in the upper and middle parts of the slope to 168 mm in its lower part. However, despite the high intensity of snow melting, visible surface runoff was absent. The snow cover disappeared due to its evaporation under the impact of solar radiation (under cloudless weather) in the afternoon, great effective radiation from the surface at night, and long-wave radiation of deep layers of snow. As a result, the upper and middle parts of the slope were completely free of snow within 3–4 days. At the same time, the soil thawed by only 0.5–1.5 cm. The snowmelt water strongly moistened the upper soil layer, which became liquid on steep parts of the slope. This caused the predomination of solifluction and creep over erosion on the slope. Thus, the results of the scanning made it possible to describe the entire range of exogenous processes affecting the soil surface, though it was difficult to differentiate between them. After heavy rains in summer, almost all landslide bodies were destroyed by rill erosion. A morphologically well-pronounced dense network of rills was formed on the surface. Their maximum width reached 15–20 cm, and their depth was up to 8–10 cm. The data obtained attested to a high intensity of exogenous processes. Accumulative

Table 2. Quantitative parameters of the rill network

Parameter	Scanning date	Sector A	Sector B
Total length of rills, m	Sept. 7, 2015	250.74	151.76
	Sept. 8, 2015	263.73	172.24
Density of rill network, m/m^2	Sept. 7, 2015	8.24	6.48
	Sept. 8, 2015	8.67	7.35

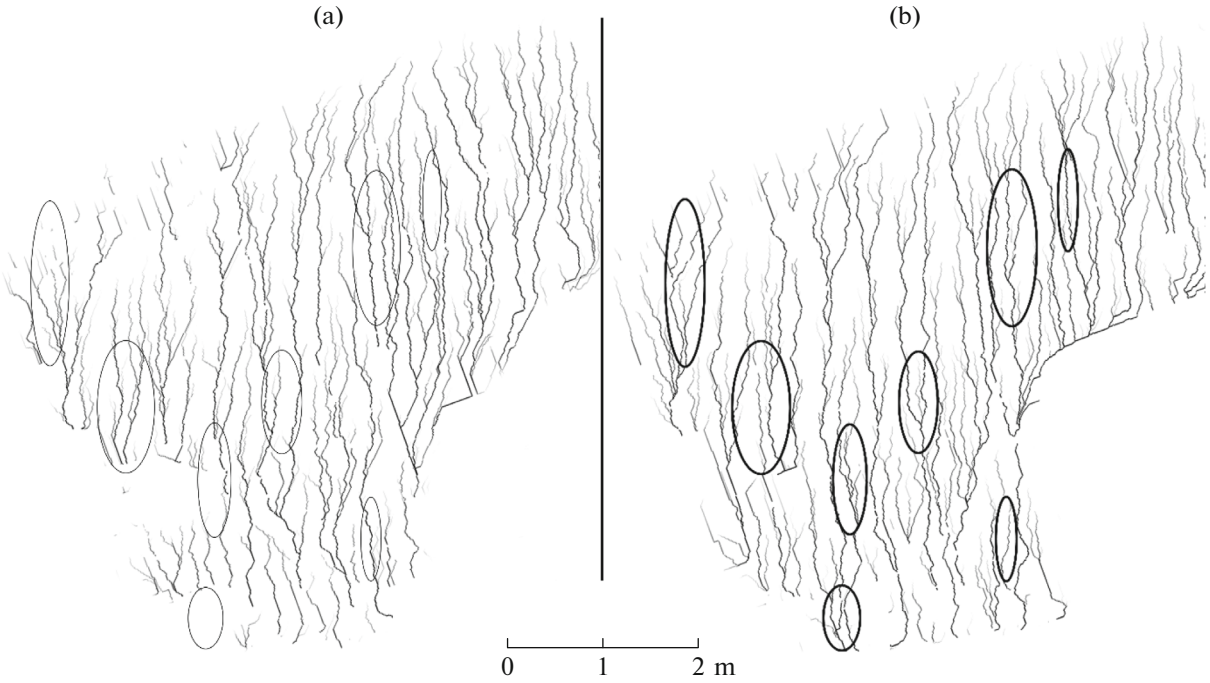

Fig. 4. Plane patterns of rills on the Kazanka plot (sector A) on (a) September 7, 2015 and (b) September 8, 2015.

processes predominated on the upper parts of sectors A and B (3.5 mm, or 57 t/ha), and denudation was the main process on the middle and lower parts (4.1 mm, or 66.1 t/ha and 4.3 mm, or 68.4 t/ha, respectively).

New quantitative data on the rates of slope erosion in the period of autumn rains were also obtained using TLS. It is generally believed that the major erosion on slopes takes place after heavy rains in summer, while it is practically absent in the fall with mainly drizzling rains. However, this aspect of erosion remains poorly studied; it is supposed that the surface runoff in autumn is minimal or absent because of the low intensity of rains [3]. In the absence of runoff-forming precipitation, erosion is not developed. Nevertheless, the TLS data indicate that the real picture is different. The leading role belongs not to the intensity of rainfall but to other parameters, such as soil moistening, vegetation cover, precipitation layer, slope morphometry, etc. For example, in autumn 2014 (September–October), a significant precipitation layer (124 mm) strongly moistened the soil. This was obviously the main factor of the development of surface runoff at rains of low intensity. The studied slope (Kazanka plot) was scanned from two stations on October 4 and 18 after several rains with a thick precipitation layer. We performed the first scanning after three rains with the total precipitation layer of more than 70 mm and the second scanning after the last autumn rain with the precipitation layer of 18.1 mm. All parts of the first sector (A) of the experimental slope were characterized by some accumulation of sediments with the average rate of 0.9 mm (about 7 t/ha). In the other sector (B), on the contrary, erosion prevailed. The mean thickness of the denuded layer reached 2.4 mm (19.4 t/ha). The accumulation on plot A was probably caused by an undulating shape of the transverse profile of the slope with lateral water inflow from the interfluve against the background of the preserved areas with the undisturbed sod layer under plants in the upper and middle parts of the slope. These areas prevented the development of surface runoff. We did not find visible changes in the system of rills on these parts of the slope. Some movement of the soil masses along the slope was due to their creep and illuviation of clay into the system of fissures (colmatage). These processes could be clearly seen on side walls of the rills.

In the period of autumn rains of 2015 (before November 23) in sector B (sector A was overgrown and excluded from the observations), the slope surface significantly changed, and erosion generally predominated on the slope. Its average intensity on the upper, middle, and lower parts of the slope was estimated at 8.8, 7.0, and 10.0 mm, respectively. Thus, upon the assessment of slope erosion, the period of autumn rains should be taken into consideration. Erosion on steep slopes with extremely moistened soil without vegetation (their areas are large after harvesting and autumn plowing) after rains of small intensity but with great precipitation layer may be even stronger than in that in the summer.

Scanning data for different periods were arranged into a geodatabase, the fragment of which is given in Table 1.

Table 3. Data of scanning after extremely heavy rain (Kazanka plot, sector B)

Kazanka plot	S, m^2	V_+	V_-	V_+-V_-	E, m^3/ha	i_+	i_-	Δi
Total plot	23.42	0.01	−0.17	−0.17	−73.28	0.22	−7.55	−7.33
Upper part	7.07	0.00	−0.05	−0.05	−70.60	0.21	−7.27	−7.06
Middle part	8.55	0.00	−0.06	−0.06	−69.40	0.15	−7.09	−6.94
Lower part	7.80	0.00	−0.06	−0.06	−76.84	0.29	−7.98	−7.68

Another methodological approach, which should be used for erosion scanning data, is the analysis of the plane pattern of the rill network. There are several reasons to perform it. It was already noted that scanning fixes all the smallest changes in micro- and nanoelements of topography. They may be related to other factors besides erosion. First, slopes (steep slopes, in particular) undergo a combination of exogenous processes (landslides, solifluction, deflation, etc.). Second, physical processes in a soil developing upon changes in the soil water content may also affect the results. Third, a particular role belongs to anthropogenic impacts, for example, a disturbance of the soil cover by agricultural machines.

Since high scanning accuracy and density may be a restriction at the interpretation of scanning data, we improved the approach to the processing of scanning data for the assessment of erosion rates. We assumed that sheet erosion is minimal, and the main soil mass is removed as a result of formation of the system of rills. A general lowering of the surface is related to spatial change in the plane patter of the system of rills after each case of surface runoff. The interrill erosion is also developed due to the impact of falling raindrops or other exogenous processes (most often, solifluction upon the snowmelt runoff). Therefore, it is necessary to take into consideration only linear washouts—rills and gullies—for the determination of the rate and dynamics of erosion by scanning. Further work implies the application of a well-known approach to erosion determination by the volume of rill washouts offered by Sobolev [7], or by various ways of photoprofiling [3]. This will make it possible to increase the accuracy and efficiency of measurements and to avoid mechanical disturbance of the surface of the studied plot. When it is necessary to determine denudation rate on slopes, changes are assessed on the entire studied surface from the cloud of points. It is necessary to make a correction for the physical status of soil, because differences in moistening exert effect on the surface height in point clouds at repeated scanning.

The changes in the plane patter of rills after runoff were analyzed with the use of the Esri ArcMap software, and the volumes of eroded material were calculated from the obtained clouds of points. These data demonstrate the changes after each runoff. For example, the pattern obtained reflects a very strong plane transformation of the system of rills on the Kazanka plot (Fig. 4). The analysis of the quantitative characteristics (Table 2) attests to a greater density of rills in sector A (8.24 m/m^2) in comparison with sector B (6.48 m/ m^2). Despite these data, erosion was stronger in sector B due to deepening of the beds of the rills.

In general, it should be mentioned that there is a tendency for straightening of microrill beds, increase in their total amount, and junction of microrills into larger rills. This results in the development of the process termed sheet erosion, at which a rather uniform layer of soil and ground is cut off. It is mainly related to the plane shift of microrills after each case of the surface runoff rather than to the sheet runoff proper.

During the survey, special attention should be paid to the extreme meteorological conditions, in particular, to heavy rains of high intensity. For example, on the Kazanka plot (sector B), a hurricane on September 7, 2015 was accompanied by extremely heavy rain with the precipitation layer of 25.1 mm (more than a half of the monthly norm). The heavy rain resulted in a strong erosion from 7 mm (70.6 m^3/ha) to 7.7 mm (76.84 m^3/ha) in the upper top middle parts of the slope, respectively. The mean eroded layer for the entire sector was 7.3 mm (73.3 m^3/ha) at the accumulation equal to 0.22 mm (Table 3). The total length and density of rills increased by 13% in sector B and by 5% in sector A (Table 2). The depth of the largest rills was 15 cm at the mean depth of only 3 cm the entire plot. The mean summer erosion for the studied sectors was 13 mm, and the accumulation comprised 7 mm. Therefore, only one extreme case of surface runoff produced more than a half of the entire soil loss volume as a result of deepening of the existing system of the rills.

The performed analysis of the dependence of the rates of erosion and accumulation of sediments on the precipitation layer has shown that the role of rainfall is considerable (from 40% to 70% at the correlation coefficient from 0.62 to 0.83, Table 4), other parameters (type of soils; projective cover of vegetation; and slope length, steepness, and aspect) being equal.

The elaborated approach to TLS was tested on plowed lands. A plot with morphologically well-pronounced network of rills, which was subdivided into two sectors (A and B), was chosen in the northeast of Kazan (Chebaksa plot). The scanning was performed two times in the period from June 30 to September 8, 2015. Precipitation amount in that period exceeded 200 mm (1.5 times higher than the norm); there were 36 days with rains. Despite the development of the rill

Table 4. Dependence of erosion (mm) on summer precipitation (Kazanka plot)

Date	Precipitation, mm	Sector A		Sector B	
		i_-	i_+	i_-	i_+
Jun. 20, 2014	33.6	−11.50	3.66	−5.21	4.69
Jul. 8, 2014	37.8	−3.76	3.66	−2.85	5.69
Jul. 21, 2014	15.2	−4.76	4.88	−3.97	2.99
Aug. 30, 2014	63.7	−7.18	5.29	−6.83	3.54
Oct. 30, 2014	84.8	−2.61	9.86	−1.57	9.15
Jun. 5, 2015	10.3	Measurements were absent in 2015 (overgrowing by grass)		−8.19	5.31
Jun 20, 2015	16.5			−12.23	1.46
Jul. 9, 2015	43.7			−4.27	5.63
Sep. 7, 2015	25.1			−7.55	0.22
Nov. 23, 2015	124.5			−13.22	4.57
η^2, correlation ratio		0.7	0.59	0.39	0.42
r, correlation coefficient		0.83	0.77	0.62	0.65

Table 5. Processed scanning data on plowed field in 2015 (Chebaksa plot)

Sector, data	S, m^2	V_+	V_-	V_+-V_-	E, m^3/ha	i_+	i_-	Δi
		m^3				mm		
A, Jun. 30–Sep. 8	4.49	0.002	0.026	0.024	53.45	5.79	0.45	5.35
B, Jun 30–Sep. 8	18.7	0.017	0.151	0.134	71.66	8.07	0.91	7.17

Table 6. Observation data on changes in volume of transported material at gully erosion in 2015–2016 (plot Shali)

Period	Gully 1					Gully 2				
	S, m^2	V_+	V_-	V_+-V_-	E, m^3/m^2	S, m^2	V_+	V_-	V_+-V_-	E, m^3/m^2
		m^3					m^3			
Spring 2016	196.71	16.97	20.94	−3.96	−0.02	66.48	1.93	7.77	−5.84	−0.09
Autumn 2016	109.31*	12.79	1.99	10.80	0.1	68.86	2.77	2.38	0.39	0.01

* Without gully mouth.

network, the accumulation of sediments predominated in both sectors: 5.79 mm (A) and 8.07 mm (B) (Table 5). Erosion was generally small: from 0.45 to 0.91 mm. This is related to the fact that the investigated plots were laid at the lower boundary of the field, where the material from the above-lying plowed slope was accumulated and sprouted perennial grasses prevented the development of erosion.

TLS of gully erosion. The instrumental monitoring of plot Shali with the use of laser scanning for the determination of the volumes of the moved material (per area and in the given points) began 2015. Only the linear growth of gullies may be estimated by conventional approaches under real terrain conditions. The transformation rates of sidewalls of gullies usually cannot be determined. This problem may be successfully solved by TLS. The data obtained are given in Table 6.

Despite different configuration, aspect, and steepness of the slopes, volumetric changes within one-year period for the gullies are comparable: 0.12 and 0.10 m^3/m^2 for gullies 1 and 2, respectively. However, the dynamics of soil transportation in them were different: denudation for the period after the snowmelt runoff for gully 2 is 1.5–2 times larger than for gully 1. The material accumulation over the period of summer and autumn rains in gully 1 is mainly related to intensive landslide processes rather than to the material transportation from the adjacent field covered by

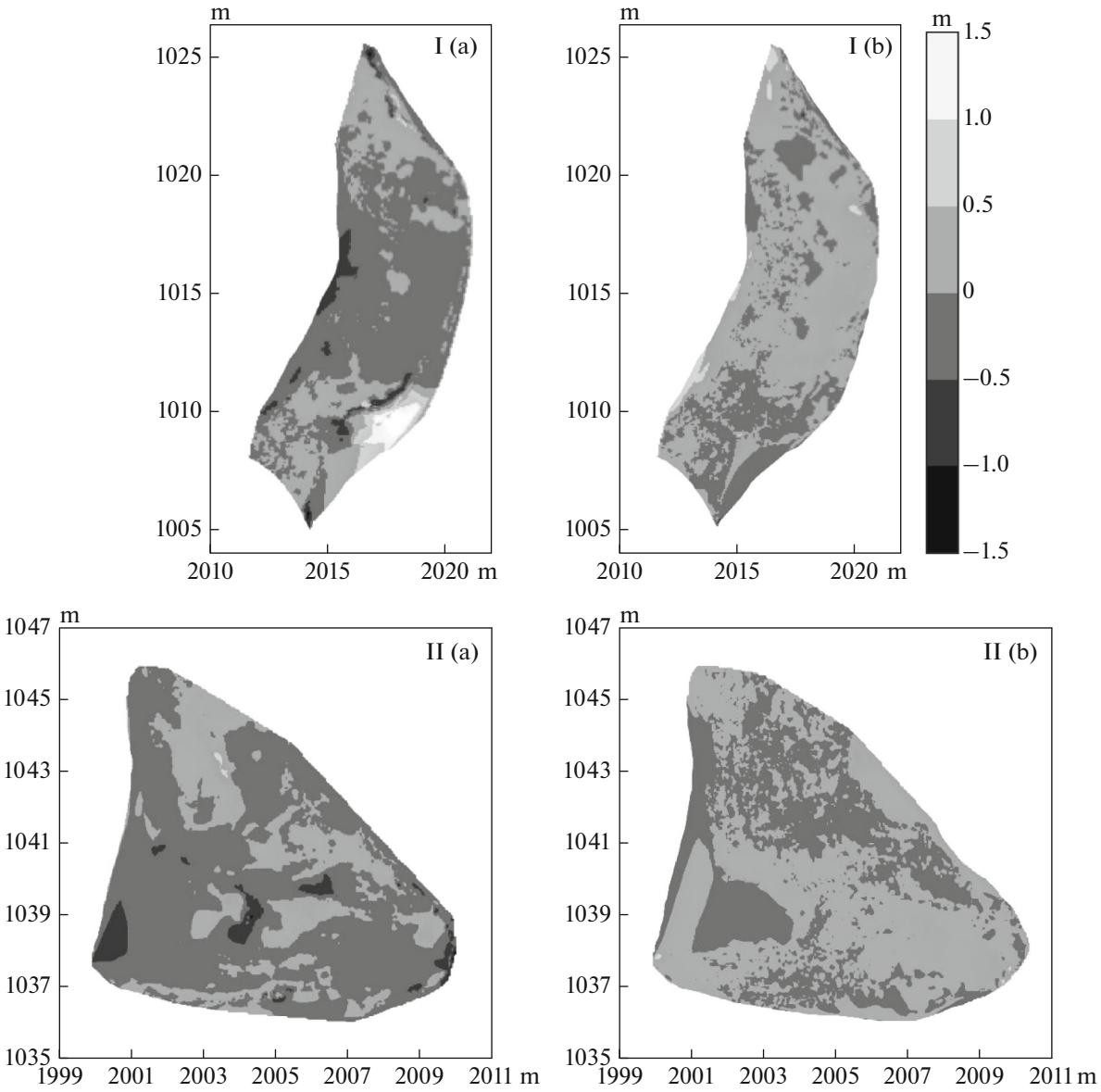

Fig. 5. Maps of surface differentiation for the periods after (a) snowmelt runoff and (b) summer–autumn rains for gully 1(I) and gully 2 (II) in conventional coordinate system.

perennial grasses. This is confirmed by the maps of surface differentiation (Fig. 5). For gully 2, volumetric changes are explained by the transportation of material eroded from the walls inside the gully and by input of material eroded from the adjacent plowed land (Fig. 6).

The use of TLS enabled us to estimate the linear growth of the upper parts of the gullies. Thus, in 2015–2016, it reached 0.45 m for gully 1 and 0.3 m for gully 2. This is confirmed by measurements with the use of benchmarks.

Thus, the TLS method provides efficient and precise estimation of not only linear and areal changes in the shape of the gullies but also of the volumes and rates of transformation of their sidewalls.

CONCLUSIONS

A new method of the quantitative assessment of the intensity of rill and gully erosion with the use of terrestrial laser scanning has been elaborated. Its high precision and speed were impossible for previous devices. The advantages of the method include identification of different types of erosion caused by temporary water streams, measurements without disturbance of the studied surface, safety of the performed measuring works, and possibility to develop high-precision digital elevation model making it possible to calculate morphometric parameters of slope (mean steepness, lengths of streamlines, curvature, aspect, etc.). This method also makes it possible to assess the denuda-

tion–accumulative balance on slopes, to determine the dynamics of the amounts of transported material in different parts of slope at various events of the surface runoff, and to identify spatial regularities of the formation of rills and gullies. It can be used for the integral evaluation of the total effect of the set of exogenous processes on slopes. The data obtained by the TLS method may play a special role in the determination of regularities of gully erosion. Using TLS on test plots, we have obtained data on the amount of eroded and accumulated material in the period of autumn rains, when intensive erosion–accumulation processes are related to the absence of grass cover, high soil moistening, and large total precipitation.

ACKNOWLEDGMENTS

This work was supported by the Russian Science Foundation, project no. 15-17-20006.

REFERENCES

1. A. M. Gafurov and B. M. Usmanov, "Evaluation of intensity and dynamics of soil erosion by terrestrial laser scanning," in *Erosion, Channel, and Estuary Processes: Research Works of Young Scientists from Universities* (Minin Univ., Nizhny Novgorod, 2016), pp. 81–90.
2. V. N. Golosov, *Erosion-Accumulative Processes in River Basins of Cultivated Plains* (GEOS, Moscow, 2006) [in Russian].
3. O. P. Yermolaev, "Geoinformation mapping of soil erosion in the Middle Volga region," Eurasian Soil Sci. **50**, 118–131 (2017).
4. O. P. Yermolaev, *The Zones of Erosion in Natural-Anthropogenic Landscapes of River Basins* (Kazan State Univ., Kazan, 1992) [in Russian].
5. M. S. Kuznetsov, G. P. Glazunov, and V. Ya. Grigor'ev, *Methods for Studying Erosion Processes* (Moscow State Univ., Moscow, 1986) [in Russian].
6. G. A. Larionov, *Erosion and Deflation of Soils: General Regularities and Quantitative Estimations* (Moscow State Univ., Moscow, 1993) [in Russian].
7. S. S. Sobolev, *Soil Erosion Control and Improvement of Soil Fertility* (Sel'khozizdat, Moscow, 1961) [in Russian].
8. A. Afana, A. Solé-Benet, and J. L. Pérez, "Determination of soil erosion using laser scanners," *Proceedings 19th World Congress of Soil Sciences "Soil Solutions for a Changing World," Brisbane, Australia* (International Union of Soil Sciences, Crawley, 2010), pp. 39–42.
9. G. Antova, "Registration process of laser scan data in the field of deformation monitoring," Procedia Earth Planet. Sci. **15**, 549–552 (2015).
10. J. Bechet, J. Duc, M. Jaboyedoff, A. Loye, and N. Mathys, "Technical note: erosion processes in black-marls at the millimetre scale, the input of an analogical model," Hydrol. Earth Syst. Sci. Discuss. **11** (2), 2263–2275 (2014).
11. J. M. Bodoque, J. A. Ballesteros-Cánovas, A. Lucía, A. Díez-Herrero, and J. F. Martín-Duque, "Source of error and uncertainty in sheet erosion rates estimated from dendrogeomorphology," Earth Surf. Process. Landforms **40** (9), 1146–1157 (2015).
12. P. Dabek, R. Zmuda, B. Ćmielewski, and J. Szczepański, "Analysis of water erosion processes using terrestrial laser scanning," Acta Geodyn. Geomater. **11** (173), 45–52 (2013).
13. S. S. Day, K. B. Gran, P. Belmont, and T. Wawrzyniec, "Measuring bluff erosion part 2: pairing aerial photographs and terrestrial laser scanning to create a watershed scale sediment budget," Earth Surf. Process. Landforms **38** (10), 1068–1082 (2013).
14. J. U. H. Eitel, C. J. Williams, L. A. Vierling, O. Z. Al-Hamdan, and F. B. Pierson, "Suitability of terrestrial laser scanning for studying surface roughness effects on concentrated flow erosion processes in rangelands," Catena **87** (3), 398–407 (2011).
15. A. Eltner and P. Baumgart, "Accuracy constraints of terrestrial Lidar data for soil erosion measurement: application to a Mediterranean field plot," Geomorphology **245**, 243–254 (2015).
16. L. Fan and P. M. Atkinson, "Accuracy of digital elevation models derived from terrestrial laser scanning data," IEEE Geosci. Remote Sens. Lett. **12** (9), 1923–1927 (2015).
17. M. Franz, D. Carrea, A. Abellán, M.-H. Derron, and M. Jaboyedoff, "Use of targets to track 3D displacements in highly vegetated areas affected by landslides," Landslides **13** (4), 821–831 (2016).
18. A. Gruen and D. Akca, "Least squares 3D surface and curve matching," ISPRS J. Photogramm. Remote Sens. **59** (3), 151–174 (2005).
19. G. R. Hancock, D. Crawter, S. G. Fityus, J. Chandler, and T. Wells, "The measurement and modelling of rill erosion at angle of repose slopes in mine spoil," Earth Surface Process. Landforms **33** (7), 1006–1020 (2008).
20. A. A. Hawdon, S. N. Wilkinson, A. E. Kinsey-Henderson, N. Goodwin, R. Bartley, and B. W. Baker, "Rapid acquisition of gully topography using a mobile, handheld laser scanner," *7th International Symposium on Gully Erosion, May 23–27, 2016* (Purdue University, Stewart Center, West Lafayette, 2016), p. 40.
21. W. Kociuba, G. Janicki, J. Rodzik, and K. Stępniewski, "Comparison of volumetric and remote sensing methods (TLS) for assessing the development of a permanent forested loess gully," Nat. Hazards **79**, 139–158 (2015).
22. W. Kociuba, W. Kubisz, and P. Zagórski, "Use of terrestrial laser scanning (TLS) for monitoring and modeling of geomorphic processes and phenomena at a small and medium spatial scale in Polar environment (Scott River–Spitsbergen)," Geomorphology **212**, 84–96 (2014).
23. L. Longoni, M. Papini, D. Brambilla, L. Barazzetti, F. Roncoroni, M. Scaioni, and V. I. Ivanov, "Monitoring riverbank erosion in mountain catchments using terrestrial laser scanning," Remote Sens. **8** (3), 241 (2016).
24. O. Monserrat and M. Crosetto, "Deformation measurement using terrestrial laser scanning data and least squares 3D surface matching," ISPRS J. Photogramm. Remote Sens. **63** (1), 142–154 (2008).

25. F. Neugirg, M. Stark, A. Kaiser, M. Vlacilova, M. Della Seta, F. Vergari, J. Schmidt, M. Becht, and F. Haas, "Erosion processes in calanchi in the Upper Orcia Valley, Southern Tuscany, Italy based on multitemporal high-resolution terrestrial LiDAR and UAV surveys," Geomorphology **269**, 8–22 (2016).
26. K. R. Olson, G. A. Larionov, and M. A. Nearing, "Evaluation of methods to quantify soil loss from erosion," *Proceedings of the International Workshop on Quantification and Assessment of Soil Erosion, September 20–24, 1993* (Moscow State Univ., Moscow, 1994), pp. 260–277.
27. J. A. Palenzuela, J. D. Jiménez-Perálvarez, R. El Hamdouni, P. Alameda-Hernández, J. Chacón, and C. Irigaray, "Integration of LiDAR data for the assessment of activity in diachronic landslides: a case study in the Betic Cordillera (Spain)," Landslides **13** (4), 629–642 (2016).
28. R. L. Perroy, B. Bookhagen, G. P. Asner, and O. A. Chadwick, "Comparison of gully erosion estimates using airborne and ground-based LiDAR on Santa Cruz Island, California," Geomorphology **118** (3–4), 288–300 (2010).
29. A. Pesci, G. Teza, G. Casula, F. Loddo, P. De Martino, M. Dolce, F. Obrizzo, and F. Pingue, "Multitemporal laser scanner-based observation of the Mt. Vesuvius crater: characterization of overall geometry and recognition of landslide events," ISPRS J. Photogramm. Remote Sens. **66** (3), 327–336 (2011).
30. T. Schmid, H. Schack-Kirchner, and E. Hildebrand, "A case study of terrestrial laser scanning in erosion research: Calculation of roughness indices and volume balance at a logged forest site," Int. Arch. Photogramm., Remote Sens. Spatial Inf. Sci. **36** (8), 114–118 (2004).
31. D. M. Staley, T. A. Wasklewicz, and J. W. Kean, "Characterizing the primary material sources and dominant erosional processes for post-fire debris-flow initiation in a headwater basin using multi-temporal terrestrial laser scanning data," Geomorphology **214**, 324–338 (2014).
32. B. Usmanov, O. Yermolaev, and A. Gafurov, "Estimates of slope erosion intensity utilizing terrestrial laser scanning," Proc. Int. Assoc. Hydrol. Sci. **367**, 59–65 (2014).
33. M. Vaaja, J. Hyyppä, A. Kukko, H. Kaartinen, H. Hyyppä, and P. Alho, "Mapping topography changes and elevation accuracies using a mobile laser scanner," Remote Sens. **3** (3), 587–600 (2011).
34. A. Vinci, R. Brigante, F. Todisco, F. Mannocchi, and F. Radicioni, "Measuring rill erosion by laser scanning," Catena **124**, 97–108 (2015).
35. X. Xu, F. Zheng, C. Qin, and H. Wu, "Active stage gully morphological characteristics in the loess hilly-gully region based on 3D laser scanning technique," *7th International Symposium on Gully Erosion, May 23–27, 2016* (Purdue University, Stewart Center, West Lafayette, 2016), pp. 24–25.

Translated by I. Bel'chenko